View metadata, citation and similar papers at core.ac.uk
brought to you by CORE
provided by Elsevier - Publisher Connector

Structure
Article

Structural Determinants of RGS-RhoGEF Signaling Critical to *Entamoeba histolytica* Pathogenesis

Dustin E. Bosch,[1] Adam J. Kimple,[1] Alyssa J. Manning,[2] Robin E. Muller,[1] Francis S. Willard,[1,4] Mischa Machius,[1] Stephen L. Rogers,[2] and David P. Siderovski[3,*]
[1]Department of Pharmacology
[2]Department of Biology
The University of North Carolina at Chapel Hill, Chapel Hill, NC 27599, USA
[3]Department of Physiology and Pharmacology, West Virginia University School of Medicine, Robert C. Byrd Health Sciences Center, Morgantown, WV 26506, USA
[4]Present address: Lilly Research Laboratories, Eli Lilly and Co., Indianapolis, IN 46285, USA
*Correspondence: dpsiderovski@hsc.wvu.edu
http://dx.doi.org/10.1016/j.str.2012.11.012

SUMMARY

G protein signaling pathways, as key components of physiologic responsiveness and timing, are frequent targets for pharmacologic intervention. Here, we identify an effector for heterotrimeric G protein α subunit (EhGα1) signaling from *Entamoeba histolytica*, the causative agent of amoebic colitis. EhGα1 interacts with this effector and guanosine triphosphatase-accelerating protein, EhRGS-RhoGEF, in a nucleotide state-selective fashion. Coexpression of EhRGS-RhoGEF with constitutively active EhGα1 and EhRacC leads to Rac-dependent spreading in *Drosophila* S2 cells. EhRGS-RhoGEF overexpression in *E. histolytica* trophozoites leads to reduced migration toward serum and lower cysteine protease activity, as well as reduced attachment to, and killing of, host cells. A 2.3 Å crystal structure of the full-length EhRGS-RhoGEF reveals a putative inhibitory helix engaging the Dbl homology domain Rho-binding surface and the pleckstrin homology domain. Mutational analysis of the EhGα1/EhRGS-RhoGEF interface confirms a canonical "regulator of G protein signaling" domain rather than a RhoGEF-RGS ("rgRGS") domain, suggesting a convergent evolution toward heterotrimeric and small G protein cross-talk.

INTRODUCTION

Heterotrimeric G protein signaling pathways are frequent targets for pharmacologic manipulation (Gilchrist, 2007). The Gα subunit in its inactive, guanosine diphosphate (GDP)-bound conformation engages the obligate Gβγ dimer (Oldham and Hamm, 2008). A ligand-activated seven-transmembrane G protein-coupled receptor promotes nucleotide exchange on the Gα subunit. Upon binding of guanosine triphosphate (GTP) by the Gα subunit, three switch regions undergo a conformational change, leading to separation from Gβγ and subsequent activation of downstream effectors, such as adenylyl cyclases, phospholipase C, and Rho-family guanine nucleotide exchange factors (RhoGEFs) (Aittaleb et al., 2010; Oldham and Hamm, 2008). Signaling is terminated by the guanosine triphosphatase (GTPase) activity of the Gα subunit and reassembly of the Gα·GDP/Gβγ heterotrimer.

"Regulator of G protein signaling" (RGS) proteins accelerate the intrinsic GTP hydrolysis activity of Gα subunits and thereby serve as negative regulators of signaling (Kimple et al., 2011). Canonical nine-helix RGS domains exhibit highest affinity for Gα in its transition-state mimetic form, stabilizing the switch regions for efficient hydrolysis (Tesmer et al., 1997). Members of the RGS-RhoGEF family of Gα effectors contain N-termini with similarity to RGS domains (called "RhoGEF-RGS" or "rgRGS" domains), in combination with Dbl homology (DH) and pleckstrin homology (PH) domains that together mediate activation of Rho family GTPases (Aittaleb et al., 2010). The DH domain engages substrate Rho GTPases, promoting nucleotide release, while the PH domain frequently modulates exchange in various Dbl-family RhoGEF members (Rossman and Sondek, 2005). In contrast to nine-helix RGS domains, rgRGS domains have a distinct 12-helix fold and engage $G\alpha_{12/13}$ subunits through an effector-like interface involving primarily switch 2 and the α3 helix (Aittaleb et al., 2010). An N-terminal extension of the rgRGS domain containing an "IIG" sequence motif contacts the $G\alpha_{12/13}$ switch regions and all-helical domain and, in the case of p115 RhoGEF, is required for GTPase accelerating protein (GAP) activity toward $G\alpha_{12/13}$ subunits. Although structures of RGS-RhoGEFs with both the rgRGS and DH-PH domain tandems have not yet been elucidated, p115 RhoGEF is thought to be activated by an allosteric "GEF switch" mechanism that involves a conformational change of an N-terminal extension of the DH domain (Chen et al., 2011). Recent low-resolution structural studies of full-length p115 RhoGEF suggest an elongated domain architecture and a potential bimodal interaction with Gα13, namely the effector interface with the rgRGS domain and a potential additional interface with the DH domain (Chen et al., 2012). The activation mechanism of another mammalian

RGS-RhoGEF, PDZ-RhoGEF, is thought to be complex, involving disruption of an electrostatic RGS-DH linker and DH domain interaction, perturbation of a putative RGS-DH linker "molten globule," and membrane recruitment, as well as a "GEF switch" (Bielnicki et al., 2011; Zheng et al., 2009). Low-resolution small-angle X-ray scattering (SAXS) studies of PDZ-RhoGEF also suggested an ensemble of elongated domain architectures (Bielnicki et al., 2011).

Entamoeba histolytica causes an estimated 50 million infections and 100,000 deaths per year worldwide, with highest incidence in countries with poor barriers between drinking water and sewage (WHO, 1997). Following ingestion of encysted *E. histolytica*, the trophozoite or amoeboid form of the parasite attaches to and destroys intestinal epithelial cells, giving rise to amoebic colitis (Ralston and Petri, 2011). Although the molecular details of signaling pathways in *E. histolytica* remain understudied, a relatively large family of Rho GTPases and Dbl family RhoGEFs are known to modulate cytoskeletal dynamics, as well as key pathogenic processes, such as trophozoite migration, extracellular matrix invasion, and killing and phagocytosis of host cells (Bosch et al., 2011a; Guillén, 1996; Meza et al., 2006).

Recently, we identified a functional heterotrimeric G protein signaling pathway in *E. histolytica*; perturbation of the Gα subunit, EhGα1, elucidated positive regulatory roles for G protein signaling in pathogenic processes, such as trophozoite migration and invasion, host cell attachment, and cell killing (Bosch et al., 2012). Overexpression of either wild-type EhGα1 or a dominant negative mutant in *E. histolytica* trophozoites resulted in altered transcription of numerous genes that have implicated multiple potential mechanisms by which G protein signaling modulates pathogenesis. From this study, a set of Rho GTPase signaling proteins, including an RGS-RhoGEF, and actin-associated proteins was observed to be differentially transcribed downstream of heterotrimeric G-proteins (Table S1 available online). We hypothesized that EhRGS-RhoGEF, like its mammalian homologs, serves as an EhGα1 effector and signals through Rho family GTPases, with important roles in *Entamoeba histolytica* pathogenesis. Here our results describe EhRGS-RhoGEF as an effector and GAP of EhGα1, with importance for *E. histolytica* motility, host cell attachment, cell killing, and cysteine protease secretion. Activation of EhRGS-RhoGEF by coexpression of constitutively active EhGα1 and EhRacC leads to Rac family GTPase-dependent cell spreading in *Drosophila* S2 cells. Furthermore, we provide a crystal structure of the full-length RGS-RhoGEF in the inactive state, elucidating its molecular architecture and likely distinct evolutionary origin relative to the mammalian RGS-RhoGEFs.

RESULTS

EhGα1 Engages an RGS-RhoGEF Effector and GTPase Accelerating Protein

The *E. histolytica* genome encodes a single classical Gα subunit effector, an RGS domain-containing RhoGEF (GenBank XP_653063; named *EhRGS-RhoGEF*) with distant similarity to the RGS-RhoGEF effectors of mammalian $G\alpha_{12/13}$ subunits (Figure S1). Transcription of *EhRGS-RhoGEF* was seen to be upregulated upon overexpression of EhGα1 in *E. histolytica* trophozoites, suggesting a functional link to heterotrimeric G protein signaling (Table S1). EhRGS-RhoGEF was purified from *E. coli* (Figure S2) and found to bind directly to EhGα1 selectively in its GDP·AlF_4^- (AMF) nucleotide state, as measured by surface plasmon resonance (Figures 1A–1D). Reciprocal immobilization experiments each indicated an ~5 μM EhGα1·AMF/EhRGS-RhoGEF dissociation constant (K_D). EhRGS-RhoGEF also interacted with the constitutively active, GTPase-deficient EhGα1 (Q189L) mutant in its GTP-bound form, although with ~20-fold lower affinity than for EhGα1·AMF ($K_D \approx 110$ μM) (Figure 1B). The EhGα1(Q189L)·GTP/EhRGS-RhoGEF binding affinity could not be precisely determined by equilibrium binding analysis, due to concentration limitations of our assay. The preference of EhRGS-RhoGEF for the AMF nucleotide state over the GTP-bound state of EhGα1 is consistent with a similar order-of-magnitude difference in p115 RhoGEF affinity for $G\alpha_{i1/13}$·AMF compared to $G\alpha_{i1/13}$·GTPγS (Chen et al., 2005). To determine whether the interaction occurs through the RGS domain of EhRGS-RhoGEF, a conserved glutamate at the predicted Gα subunit-binding surface was mutated to lysine (E39K; Figure S1). Despite proper global folding of the E39K mutant (Figure S2B), it exhibited drastically reduced affinity for EhGα1·AMF (Figure 1D). The isolated RGS domain of EhRGS-RhoGEF could not be produced from *E. coli*. However, the RGS domain expressed in HEK293T cells was seen to specifically coprecipitate with purified EhGα1·AMF and EhGα1(Q189L)·GTP, but not EhGα1·GDP (Figure S2C), suggesting that the RGS domain alone is sufficient to bind EhGα1.

The relatively high affinity of wild-type EhRGS-RhoGEF for the hydrolysis transition state-mimetic (AMF) form of EhGα1 suggested that the RGS domain of EhRGS-RhoGEF may serve as a GAP for EhGα1. Interestingly, EhRGS-RhoGEF lacks the N-terminal extension containing the IIG motif that is required for the GAP activity of p115 RhoGEF (Figure S1; Aittaleb et al., 2010). However, single turnover GTP hydrolysis assays demonstrated that wild-type EhRGS-RhoGEF, but not the EhRGS-RhoGEF(E39K) mutant, accelerates the intrinsic GTP hydrolysis activity of EhGα1 in a concentration-dependent fashion (Figure 1E). Mutation of the conserved Asn-83 in the EhRGS-RhoGEF RGS domain, predicted to contact and orient EhGα1 switch residues for efficient catalysis of GTP hydrolysis (Tesmer et al., 1997), also eliminated GAP activity (Figure 1F) and dramatically reduced EhRGS-RhoGEF/EhGα1 binding affinity (Figure 1C).

EhGα1 and EhRacC Activate EhRGS-RhoGEF to Promote Rho-Dependent Cell Spreading

To determine the ability of EhRGS-RhoGEF to modulate Rho-dependent cellular processes and its potential regulation by EhGα1, we utilized *Drosophila* S2 cells that undergo a dramatic morphological transition with distinctive reorganization of actin structures when Rho family GTPases are activated by various stimuli (Rogers et al., 2003). For example, overexpression of a GTPase-deficient and constitutively active *D.m.* Rac1(G14V) leads to cell spreading in ~80% of S2 cells on a polylysine coated surface, as compared to ~20% of cells expressing red fluorescent protein (Figures 2A and 2B). Expression of constitutively active EhGα1(Q189L) and EhRGS-RhoGEF was not sufficient to significantly increase cell spreading. However, additional expression of constitutively active EhRacC(Q65L) lead to spreading,

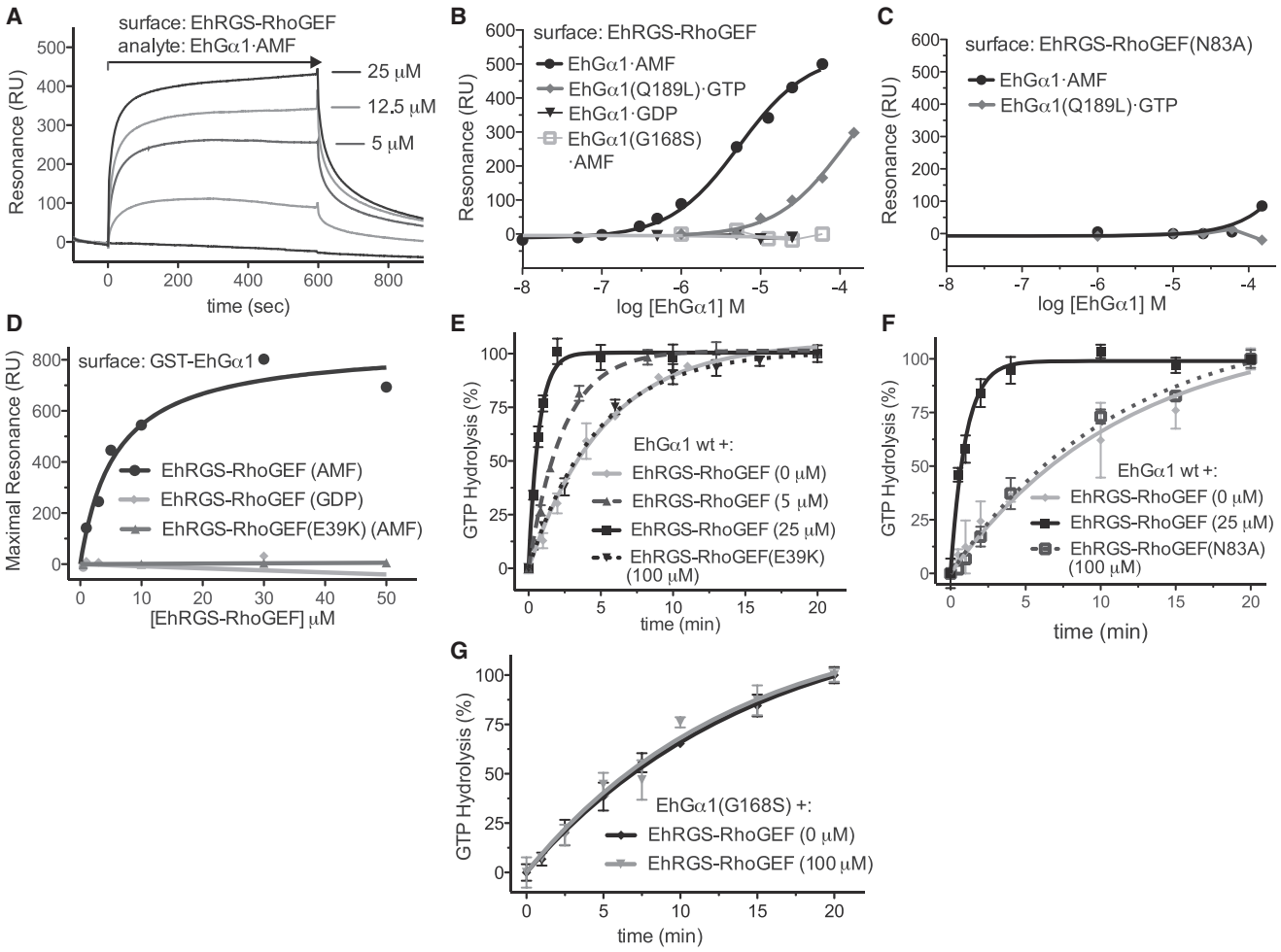

Figure 1. EhRGS-RhoGEF Is an EhGα1 Effector that Accelerates Its GTP Hydrolysis

(A–D) Either EhGα1 or EhRGS-RhoGEF was immobilized on a surface plasmon resonance chip and the complementary protein flowed over at increasing concentrations. EhRGS-RhoGEF bound EhGα1 selectively in the GDP·AlF_4^--bound state (AMF); interaction affinity was independent of immobilized species ([B] K_D = 5.2 ± 0.8 μM; [D] 5.7 ± 1.6 μM). The GTPase-deficient mutant EhGα1(Q189L) also interacted with EhRGS-RhoGEF, but with lower affinity (K_D ≈ 110 μM). Mutation of the conserved EhRGS-RhoGEF Asn-83, predicted to orient EhGα1 residues for rapid GTP hydrolysis, the predicted EhGα1-binding surface charge reversal EhRGS-RhoGEF(E39K), and the switch 1 mutant EhGα1(G168S) all drastically reduced binding affinity. Sensorgrams and equilibrium binding curves are representative of three experiments.

(E and F) The GTPase rate of EhGα1 was accelerated by EhRGS-RhoGEF in a dose-dependent fashion (k_{obs} = 0.20 ± 0.02 min^{-1} for EhGα1 alone and 1.45 ± 0.13 min^{-1} upon addition of 25 μM EhRGS-RhoGEF). EhRGS-RhoGEF(E39K) and EhRGS-RhoGEF(N83A) had no effect on the hydrolysis rate.

(G) GTP hydrolysis rates for the "RGS-insensitivity" mutant EhGα1(G168S) alone or in the presence of a high concentration of EhRGS-RhoGEF were indistinguishable. Error bars represent standard error of the mean for duplicate reactions. Each single turnover hydrolysis experiment was independently repeated at least twice.

Figure S2 indicates proper folding of the EhRGS-RhoGEF(E39K) mutant and nucleotide state-specific binding of EhGα1 to the isolated RGS domain.

suggesting that GTP-bound EhGα1 and EhRacC are necessary to activate EhRGS-RhoGEF. Importantly, EhRacC(Q65L) alone (not shown) or in combination with EhGα1 (Figure 2) did not trigger S2 cell spreading, indicating its inability to productively engage the endogenous *D.m.* Rho GTPase signaling machinery independently of EhRGS-RhoGEF. Wild-type EhGα1 did not activate EhRGS-RhoGEF, and the EhRGS-RhoGEF(E39K) mutation prevented an increase in cell spreading (Figures 2A and 2B). Thus, coexpression of EhRGS-RhoGEF with constitutively active EhRacC and interaction with constitutively active EhGα1 at the RGS domain are required for enhanced cell spreading.

The observed cell-spreading phenotype strongly suggested that EhRGS-RhoGEF was signaling through endogenous *Drosophila* Rho family GTPases. To investigate the dependence of the observed phenotype on endogenous Rho family GTPases, we knocked down expression of *D.m.* Rac1/2 (both isoforms targeted), Rho, and mtl by RNA interference, as demonstrated previously in S2 cells (Rogers and Rogers, 2008). Specific knock down of *D.m.* Rac GTPases abolished the cell-spreading effect of EhRGS-RhoGEF, EhGα1(Q189L), and EhRacC(Q65L), suggesting that either or both *D.m.* Rac isoforms may serve as substrates for overexpressed EhRGS-RhoGEF (Figure 2A).

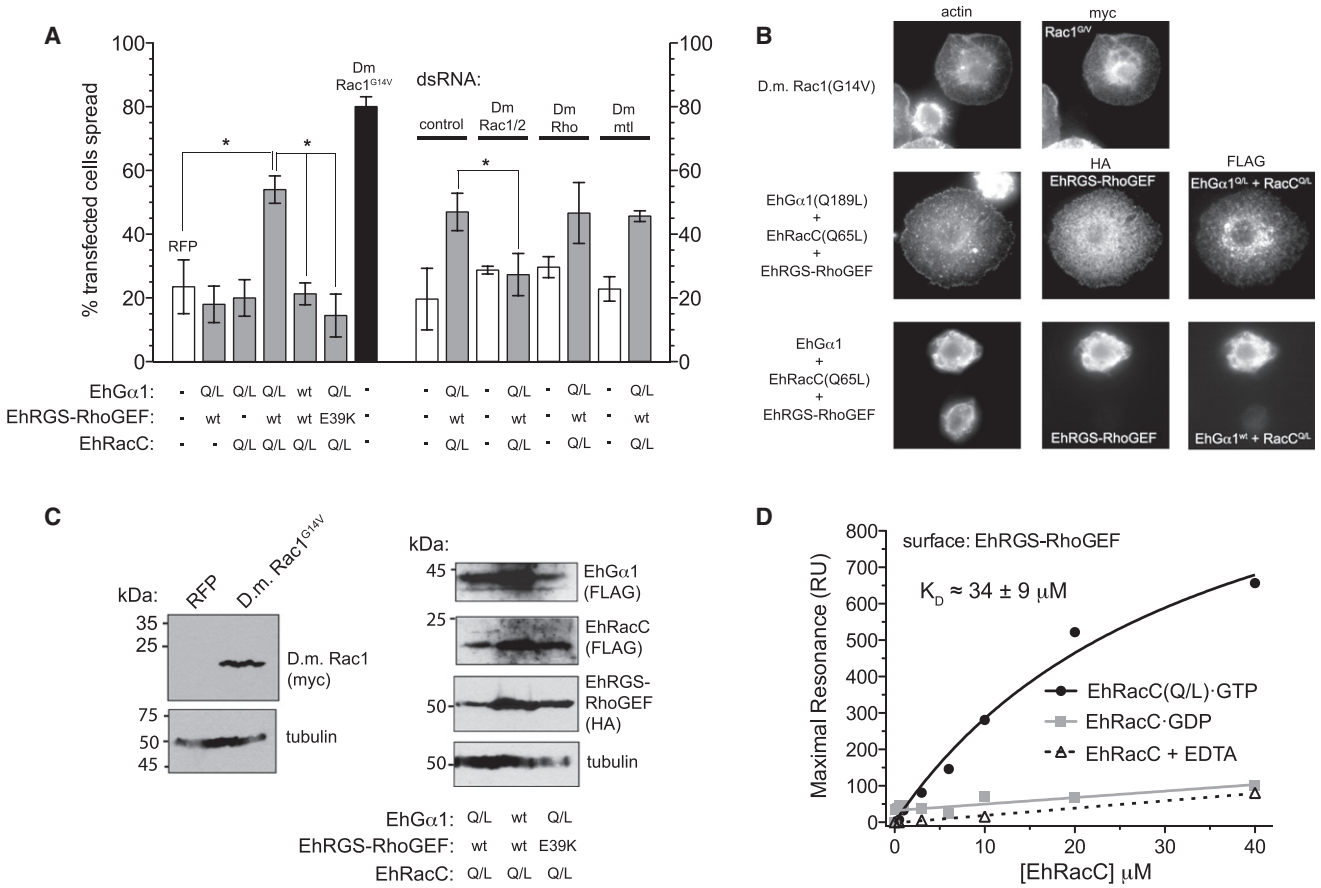

Figure 2. EhRGS-RhoGEF Activation by Constitutively Active EhGα1 and EhRacC Leads to Rac-Dependent S2 Cell Spreading

(A–C) Rho family GTPase activation in *D. melanogaster* S2 cells leads to spreading on a polylysine coated surface (Rogers and Rogers, 2008). Coexpression of EhRGS-RhoGEF with GTPase-deficient and constitutively active EhGα1(Q189L) was insufficient to effect cell spreading. However, expression of the constitutively active EhRacC(Q65L) together with EhGα1(Q189L) and EhRGS-RhoGEF significantly enhanced cell spreading, while EhRacC(Q65L) alone or in combination with EhGα1 had no effect. To determine which *D. melanogaster* Rho family GTPases were necessary for cell spreading, and thus potential substrates for overexpressed EhRGS-RhoGEF, double-stranded RNAi was employed as described previously (Rogers et al., 2003). RNAi-mediated knockdown of *D.m*. Rac isoforms, but not Rho or mtl, prevented significant enhancement of cell spreading by coexpression of EhRGS-RhoGEF, EhRacC(Q65L), and EhGα1(Q189L). Error bars represent standard deviation for three independent experiments, and * indicates statistically significant difference ($p < 0.05$) by Student's t test. Example micrographs are shown in (B) and western blots confirming expression of all *E. histolytica* proteins and mutants are shown in (C).

(D) Recombinant, activated EhRacC(Q65L)·GTP was seen to directly bind EhRGS-RhoGEF by surface plasmon resonance, while EhRacC·GDP and nucleotide-free EhRacC exhibited negligible binding up to 40 μM concentration.

Figure S1 contains sequence alignments of EhRGS-RhoGEF and mammalian homologs.

To test whether activated EhRacC directly engages EhRGS-RhoGEF, surface plasmon resonance was utilized. EhRGS-RhoGEF selectively bound EhRacC(Q65L)·GTP, to the exclusion of EhRacC·GDP or nucleotide-free EhRacC (Figure 4D). This pattern of nucleotide state selectivity was consistent with a Rho GTPase and effector-like interaction, rather than a RhoGEF and substrate Rho GTPase relationship. Although the observed recombinant EhRacC(Q65L)/EhRGS-RhoGEF affinity was relatively low ($K_D \approx 34 \pm 9$ μM), the cell-spreading experiments suggest that a productive interaction occurs in a cellular context. The interaction of EhRGS-RhoGEF with an active species of Rho family GTPase was reminiscent of the structurally elucidated interaction between human RhoA·GTPγS and a hydrophobic patch on the PH domain of PDZ-RhoGEF (Chen et al., 2010b). An analysis of the PDZ-RhoGEF PH domain residues involved in activated RhoA binding (Protein Data Bank [PDB] 3KZ1) revealed poor conservation with the corresponding PH domain residues of EhRGS-RhoGEF (19% identity, 25% similarity); thus, we do not predict that EhRacC·GTP binds EhRGS-RhoGEF in a similar fashion. However, a direct interaction does occur between activated EhRacC and EhRGS-RhoGEF, potentially explaining the required coexpression of EhRacC(Q65L), together with EhGα1(Q189L) and EhRGS-RhoGEF to enhance cell spreading (Figures 2A and 2B).

EhRGS-RhoGEF Modulates Pathogenic Processes of *E. histolytica* Trophozoites

We next investigated the role(s) of RGS-RhoGEF signaling in *E. histolytica* trophozoites by engineering the virulent HM-1:IMSS strain to stably overexpress wild-type EhRGS-RhoGEF (Figure 3). We focused on measuring the effect of EhRGS-RhoGEF overexpression on trophozoite chemotactic migration,

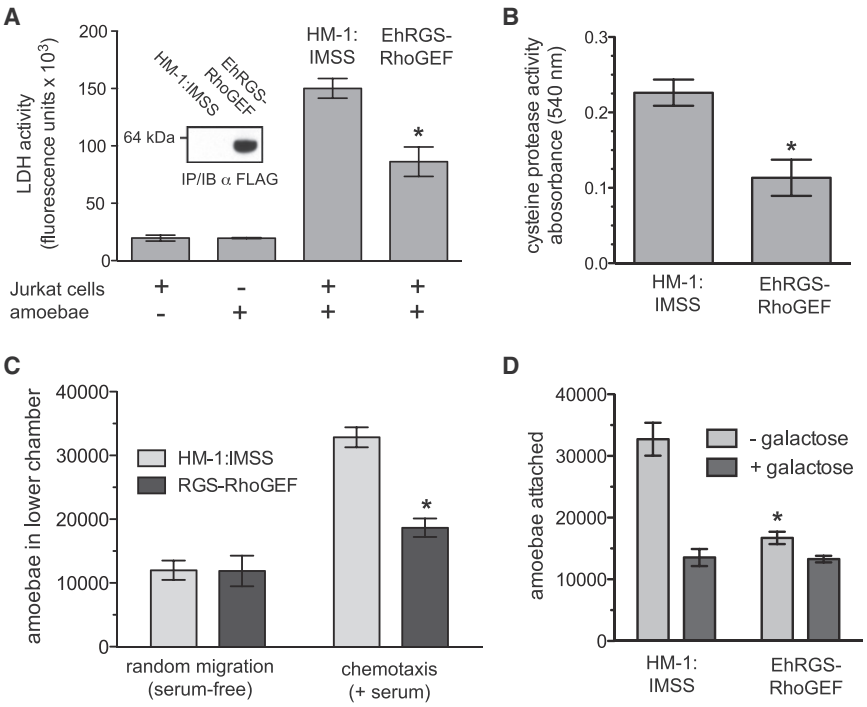

Figure 3. EhRGS-RhoGEF Expression Inhibits Host Cell Attachment and Killing, Cysteine Protease Secretion, and Chemotactic Migration by *E. histolytica* Trophozoites

(A) Amoebae were stably transfected to overexpress EhRGS-RhoGEF (inset). Expression of EhRGS-RhoGEF reduced the ability of *E. histolytica* to kill Jurkat (human lymphocyte-derived) cells compared to the HM-1:IMSS virulent parent strain, as determined by a membrane integrity assay.

(B) Trophozoites expressing EhRGS-RhoGEF exhibited reduced cysteine protease secretion, a process necessary for host cell killing and extracellular matrix invasion.

(C) Overexpression of RGS-RhoGEF reduced trophozoite chemotactic migration across a porous membrane toward serum-containing nutritive media, but had no measureable effect on random migration.

(D) Trophozoites attach to CHO cell monolayers, primarily through a galactose-inhibitable lectin. Overexpression of EhRGS-RhoGEF reduced lectin-dependent monolayer attachment. All trophozoite experiments were conducted in quadruplicate. Error bars represent standard error of the mean. * indicates a statistically significant difference by Student's t test ($p < 0.05$).

Table S1 indicates transcriptional regulation of EhRGS-RhoGEF in amoebae overexpressing EhGα1 and mutants.

host cell attachment, and cell killing, given the known dependence of these vital pathogenic processes on actin cytoskeletal dynamics, as well as Rho GTPases and Dbl family RhoGEFs (Guillén, 1996; Meza et al., 2006). Trophozoites ectopically overexpressing EhRGS-RhoGEF killed host cells less efficiently than the parent strain, as indicated by a membrane integrity assay (Figure 3A). A number of cytotoxic proteins are involved in host cell killing, including membrane-perforating amoebapores and cysteine proteases (Ralston and Petri, 2011). Reduced secretion of active cysteine proteases, as measured by an azo-collagen assay (Figure 3B), may account in part for the impaired cell killing of the EhRGS-RhoGEF-expressing trophozoite strain. Direct attachment of *E. histolytica* trophozoites to host epithelial cells, primarily through a galactose-inhibitable lectin (Petri et al., 2002), is also required for tissue destruction. Amoebae overexpressing EhRGS-RhoGEF showed reduced attachment to Chinese hamster ovary (CHO) cell monolayers compared to the parent strain (Figure 3D). *E. histolytica* trophozoites are also highly motile, a feature that is dependent on a dynamic actin cytoskeleton regulated by Rho family GTPase signaling (Meza et al., 2006). Transwell migration experiments indicated that overexpression of EhRGS-RhoGEF also decreases trophozoite chemotactic migration toward serum, but not random migration (Figure 3C), suggesting that interfering with the EhGα1/EhRGS-RhoGEF signaling axis modulates the *E. histolytica* migratory response to serum factors.

A Crystal Structure of EhRGS-RhoGEF

While isolated domains from mammalian RGS-RhoGEFs have been structurally characterized (Aittaleb et al., 2010), a high-resolution structure of an RGS domain together with a DH-PH domain tandem has not been elucidated to date. We obtained a crystal structure of a nearly full-length EhRGS-RhoGEF protein (lacking only two residues from each terminus) to 2.3 Å by single wavelength anomalous dispersion (SAD) (Table 1). The structural model exhibits an N-terminal, canonical nine-helix RGS domain, an oblong DH domain, and a C-terminal PH domain (Figure 4A). The RGS domain interacts with the DH domain surface opposite from the PH domain and the putative Rho GTPase binding site (Figure 4). The linker between the RGS and DH domains wraps around the oblong helical bundle of the DH domain (Figure 4A), forming an additional helix (termed the "inhibitory helix").

The RGS domain of EhRGS-RhoGEF is involved in multiple crystal contacts (Figure S5); specifically, the putative Gα-binding surfaces of neighboring EhRGS-RhoGEF molecules in the crystal lattice contact one another. Although crystal contacts may modestly affect the disposition of the RGS domain, the similarity of its conformation to mammalian RGS domains in both crystallographic and nuclear magnetic resonance studies (Figure 6B; Soundararajan et al., 2008) and significant burial of hydrophobic surface area (~850 Å^2) at the RGS-DH domain interface suggest that the crystal structure architecture accurately reflects that of EhRGS-RhoGEF in solution.

The PH domain exhibits a conserved overall fold despite weak sequence similarity (2.9 Å root-mean-square deviation [rmsd] compared to 324 equivalent residues of the Dbs PH domain with only 51% sequence similarity) (Figure S3A). An analysis of protein sequence motifs and comparison of the EhRGS-RhoGEF PH domain structure to other PH domains in complex with phospholipid head groups (Ferguson et al., 2000) revealed poor conservation of a potential phospholipid-binding site on EhRGS-RhoGEF. Thus, we do not hypothesize

Table 1. Data Collection and Refinement Statistics for Selenomethionine EhRGS-RhoGEF

	EhRGS-RhoGEF
PDB accession code	4GOU
Data Collection	
Space group	C2
Cell dimensions	
a, *b*, *c* (Å)	86.1, 46.3, 142.6
α, β, γ (°)	90, 104.2, 90
Peak	
Wavelength (Å)	0.97954
Resolution (Å)	43.0–2.30 (2.32–2.30)[a]
No. unique reflections	46,832
R_{merge} (%)	8.9 (58.4)[b]
$I / \sigma I$	18.5 (2.0)
Completeness (%)	98.8 (86.4)
Redundancy	4.3 (2.5)
Wilson *B*-factor (Å^2)	25.6
Refinement	
Resolution (Å)	43.0–2.30 (2.35–2.30)
No. reflections	46,587 (2,639)
R_{work}/R_{free} (%)	18.2/23.6 (26.5/32.0)
No. atoms	4,357
Protein	4,363
Ligand/ion	0
Water	216
B-factors (Å^2)	
Protein	32.5
Ligand/ion	–
Water	32.5
rmsds	
Bond lengths (Å)	0.008
Bond angles (°)	1.080

[a]Values in parentheses are for highest-resolution shell.
[b]All data were collected from a single crystal.

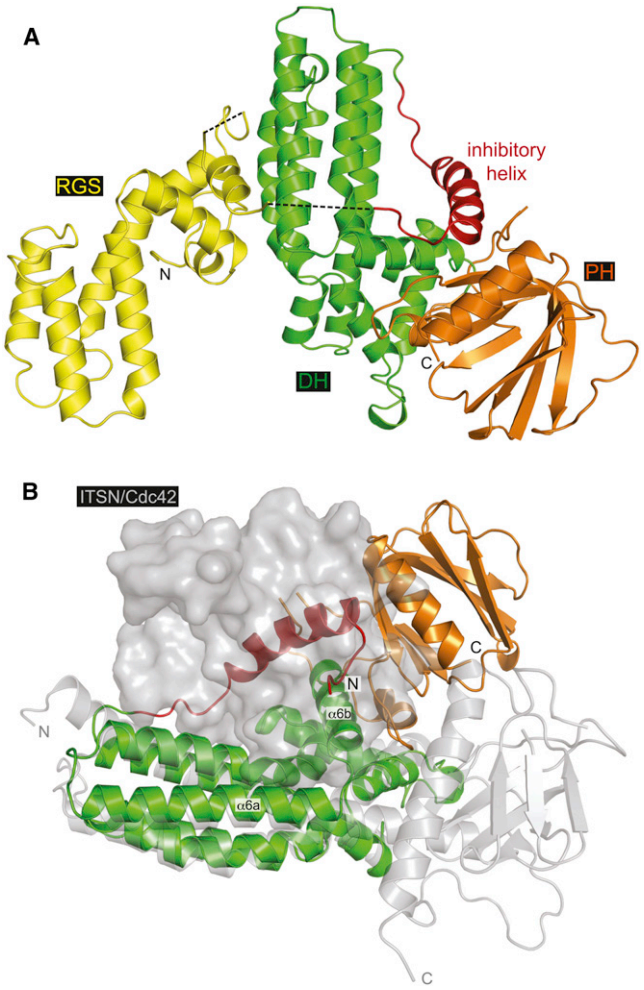

Figure 4. The Structure of EhRGS-RhoGEF Reveals Interrelationship between RGS and DH/PH Domains

(A) The RGS domain (yellow) adopts a canonical nine-helix fold and interacts with the DH domain (green) opposite from the predicted Rho binding site. The linker between the RGS and DH domains wraps ~180° around the DH domain and contains a 15-residue α helix (termed the "inhibitory helix"; red) that engages both the conserved PH domain fold (orange) and the C-terminal portion of the DH domain.

(B) The inhibitory helix, DH, and PH domains are superimposed with the structure of Intersectin/Cdc42 (gray; PDB 1KI1). The conserved site of Rho GTPase interaction, illustrated by a surface rendering of Cdc42, is obstructed in the case of EhRGS-RhoGEF. The inhibitory helix lies entirely within the space corresponding to Cdc42. In addition, the long α6 helix is continuous in Intersectin and other RhoGEFs, but is segmented into two helices related by an ~90° angle in EhRGS-RhoGEF. The α6b helix both interacts with the putative inhibitory helix and contributes to obstruction of the Rho binding site. The EhRGS-RhoGEF PH domain is also predicted to interfere with Rho binding in this inactive conformation.

Figure S3 contains an analysis of the PH domain and its DH domain interface.

that the EhRGS-RhoGEF PH domain directly associates with phospholipids.

The EhRGS-RhoGEF DH domain is most similar to that of intersectin (Dali server Z-score 19.4; PDB 1KI1). Superposition of Intersectin/Cdc42 (Snyder et al., 2002) and EhRGS-RhoGEF highlights a number of DH domain structural differences (Figure 4B). The α6 helix of EhRGS-RhoGEF, which is the longest of the Intersectin DH domain, is disrupted by a loop, giving rise to two helices at ~90° relative orientations (termed α6a and α6b). The PH domain adopts a very different orientation relative to the DH domain in EhRGS-RhoGEF as compared to Intersectin (Figure 4B). The PH domain of RGS-RhoGEF directly obstructs the putative Rho binding site, similar to a number of mammalian RhoGEFs, e.g., Vav and Sos (Das et al., 2000). The DH and PH domains of EhRGS-RhoGEF share a substantial interface (~1200 Å^2 buried surface area) that occurs predominantly through hydrophobic interactions between the α7 helix of the PH domain and the α3d, α4, α5, and α6b helices of the DH domain (Figure S3B). Particularly, the hydrophobic side chains of Phe-393 and Met-397 project into an approximately triangular concavity formed by helices α3d, α4, and α5 (Figure S3B). The nature of the DH/PH domain interface suggests that the structural relationship between the two domains observed in the crystal structure likely also exists in solution. However, additional

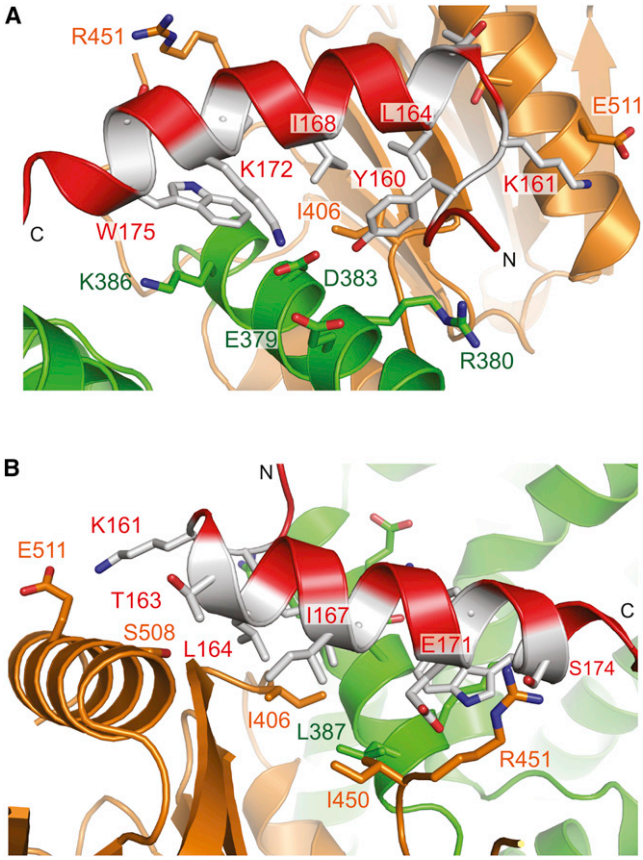

Figure 5. The EhRGS-RhoGEF Inhibitory Helix Engages Both the DH and PH Domains

(A and B) The EhRGS-RhoGEF DH and PH domains share an interface with the hydrophobic inhibitory helix residues Leu-164, Ile-167, Ile-168, Trp-175, and the aromatic ring of Tyr-160 (gray sticks). Hydrogen-bond interactions and peripheral ionic interactions, e.g., Lys-172·Asp-383 and Lys-161·Glu-511, also contribute to this interface. N and C indicate the N- and C-terminal ends of the inhibitory helix, respectively.

A $2F_o$-F_c electron density map of the inhibitory helix is shown in Figure S4.

contacts of each domain with the inhibitory helix may also be necessary to maintain the observed DH and PH domain relationship (Figure 5), and alternative conformations are also possible.

The Inhibitory Helix Coordinates Occlusion of the Rho GTPase Binding Site

In the inactive state of EhRGS-RhoGEF, the inhibitory helix, the α6b helix of the DH domain, and the PH domain all obstruct the presumptive Rho GTPase interaction surface of the DH domain (Figure 4), as predicted based on comparison with the Intersectin/Cdc42 structure (Snyder et al., 2002). In fact, the entire RGS-DH domain linker inhibitory helix lies within the space occupied by the Rho GTPase substrate in numerous, well-conserved Dbl family GEF/Rho interactions (Rossman and Sondek, 2005). The inhibitory helix interacts with both the DH and PH domains through a series of hydrophobic and polar interactions (Figure 5 and S4). The hydrophobic residues Leu-164, Ile-167, Ile-168, and Trp-175 interface with a hydrophobic patch at the DH α6B helix/PH domain interface, consisting primarily of the hydrophobic portion of Lys-386, Leu-387, Ile-406, and Ile-450 (Figure 5 and S4). Surrounding the hydrophobic patch are a number of apparent polar and ionic interactions, including those between Lys-161 of the inhibitory helix and Glu-511 of the PH domain as well as Lys-172 and Asp-383 of the inhibitory and DH domain α6B helices, respectively. The inhibitory helix residues Lys-166 and Ile-170 also form limited contacts with a DH domain loop from a neighboring molecule in the crystal lattice (Figure S5C), but these contacts likely do not contribute to the observed main chain conformation. Notably, the RGS-DH linker containing the putative inhibitory helix is much shorter in EhRGS-RhoGEF (26 residues) than the corresponding linker in its mammalian homologs, with p115 RhoGEF possessing the next shortest linker at 164 residues (Figure S1C). Thus, it is likely that this region exhibits different structural features and potentially performs different functions in mammalian RGS-RhoGEFs.

Convergent Evolution of the EhGα1/EhRGS-RhoGEF Interface

The RGS/DH domain interface consists of a central hydrophobic region with peripheral hydrogen bond and ionic interactions (Figure 6A and S4B). The residues corresponding to this domain interface are not highly conserved among mammalian RGS-RhoGEFs, such as p115 RhoGEF (Figure S1). This observation, together with a previous SAXS analysis of the elongated p115 RhoGEF (Chen et al., 2012), suggests that the structural relationships among the EhRGS-RhoGEF domains differ from those of mammalian homologs.

The RGS domain of EhRGS-RhoGEF closely resembles the nine-helix bundle found in canonical RGS domains, such as RGS4 (Figure 6B). This canonical RGS domain fold is distinct from the 12-helix rgRGS domains of mammalian RGS-RhoGEFs, such as p115 (Figure 6C; Aittaleb et al., 2010). EhRGS-RhoGEF is unique in possessing a canonical nine-helix RGS domain, suggesting that the RGS and DH-PH domain combination within *E. histolytica* may have arisen through an independent evolutionary mechanism.

In addition to possessing a distinctive RGS domain fold, the mammalian RGS-RhoGEFs engage $G\alpha_{12/13}$ subunits through an effector-like interface, primarily utilizing switch 2 and the α3 helix on Gα, although the N-terminal extension of the rgRGS domain required for GAP activity also contacts the three switches and the all-helical domain (Figure 7B; Aittaleb et al., 2010). In contrast, canonical nine-helix RGS domains primarily interface with Gα switches 1 and 2 (Figure 7A; Soundararajan et al., 2008); hence, the Gα subunit switch 1 Gly-to-Ser "RGS-insensitivity" mutation selectively disrupts canonical RGS domain interactions, but not Gα/rgRGS domain interactions (Lan et al., 1998; Meigs et al., 2005). To test whether the EhRGS-RhoGEF RGS domain interfaces with EhGα1 in a canonical fashion, we generated the EhGα1(G168S) mutant. EhRGS-RhoGEF exhibited drastically lower affinity for EhGα1(G168S) than wild-type EhGα1, as measured by surface plasmon resonance, and was unable to affect the intrinsic GTPase rate of EhGα1(G168S) (Figures 1B and 1G). These experiments suggest that the EhGα1/EhRGS-RhoGEF interface most likely resembles a canonical RGS/Gα interaction, providing further evidence for an independent evolutionary mechanism giving rise to a Gα/RGS-RhoGEF signaling axis in *E. histolytica*.

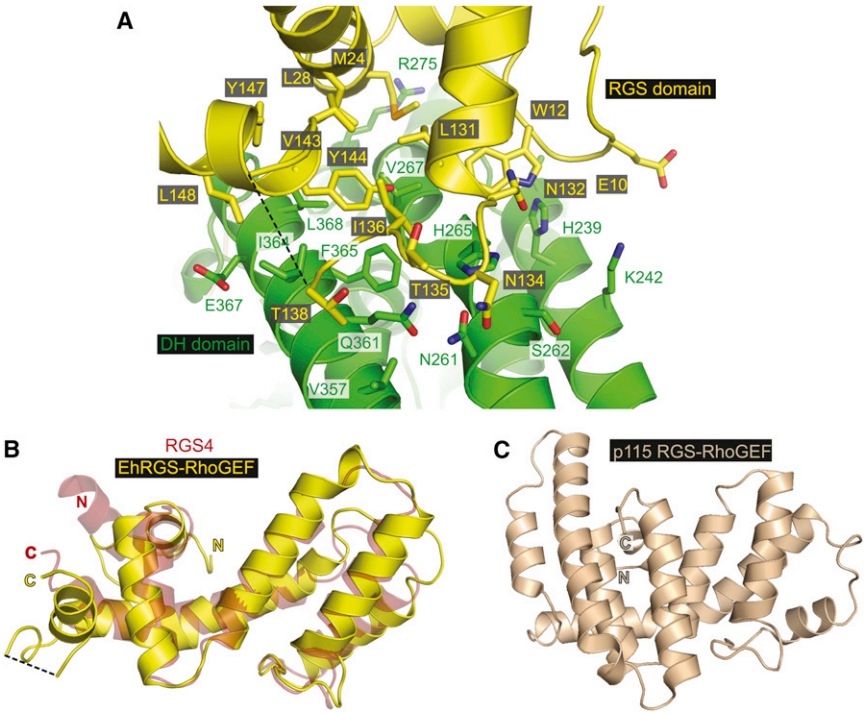

Figure 6. The EhRGS-RhoGEF RGS Domain Adopts a Canonical Fold and Interacts with the DH Domain

(A) Residues participating in the RGS (yellow) and DH (green) domain interface in EhRGS-RhoGEF are shown in sticks. A central hydrophobic region is surrounded by polar and ionic side chain interactions. A $2F_o$-F_c electron density map of the RGS/DH interface is shown in Figure S4B.

(B) The EhRGS-RhoGEF RGS domain adopts a nine-helical bundle fold very similar to canonical RGS domains, typified by RGS4 (red; PDB 1AGR).

(C) In contrast, the mammalian RGS-RhoGEFs possess an RGS-like domain with 12 helices, as seen in p115 RGS-RhoGEF (PDB 1IAP). Dotted lines indicate loops that could not be accurately modeled.

Figure S5 illustrates crystal contacts of the RGS domain and inhibitory helix.

DISCUSSION

The *E. histolytica* Gα subunit is divergent in its amino acid sequence as compared to mammalian Gα subunits and, in particular, does not belong to the $G\alpha_{12/13}$ subfamily that couples to mammalian RGS-RhoGEFs (Figure S6). However, EhGα1 does engage the RGS domain of EhRGS-RhoGEF in a nucleotide state-dependent fashion, resulting in accelerated GTP hydrolysis. A search of publicly available sequenced genomes identified the RGS and DH-PH tandem domain combination exclusively in metazoan species (e.g., *C. elegans* and *D. melanogaster*) with the only nonmetazoan exception being the *Entamoeba* species. Resistance of EhGα1 to conventional Gα subfamily classification, the RGS4-like nine-helix RGS domain fold of the EhRGS-RhoGEF N terminus, and the canonical nature of the EhGα1/EhRGS-RhoGEF interface, as evidenced by the EhGα1(G168S), EhRGS-RhoGEF(N83A), and EhRGS-RhoGEF(E39K) mutants, all suggest an evolutionary origin independent of the $G\alpha_{12/13}$/RGS-RhoGEF signaling axis present in mammals.

Mammalian RGS-RhoGEFs are thought to achieve full activation through integration of multiple signals, including, but not limited to, interactions with $G\alpha_{12/13}$. For instance, $G\alpha_{12}$-mediated stimulation of leukemia-associated RhoGEF requires tyrosine phosphorylation by Tec (Suzuki et al., 2003). Consistent with this theme, EhRGS-RhoGEF requires coexpression, not only with constitutively active EhGα1, but also with constitutively active EhRacC, to achieve apparent activation, as evidenced by S2 cell spreading. Little is currently known about EhRacC signaling in *E. histolytica*, although it is evidently a substrate for EhGEF2 in vitro (González De la Rosa et al., 2007). EhRacC was seen to bind EhRGS-RhoGEF directly, exclusively in the GTP-bound conformation, suggesting that EhRGS-RhoGEF may serve as an EhRacC effector. Activated human RhoA GTPase has been demonstrated to bind the PH domain of PDZ-RhoGEF in an analogous fashion (Chen et al., 2010b). RhoA also serves as a substrate for PDZ-RhoGEF-mediated exchange, suggesting a possible mode of feedback regulation in mammals. However, there is currently no evidence that EhRacC is a substrate for EhRGS-RhoGEF; in fact, EDTA-treated, nucleotide-free EhRacC did not bind appreciably to EhRGS-RhoGEF (Figure 2D). However, the full-length, isolated EhRGS-RhoGEF used in these experiments is expected to have an obstructed Rho substrate-binding site, and activation by EhGα1·GTP, EhRacC·GTP, and/or other factors may be required to allow efficient substrate binding. Although the putative exchange factor activity of EhRGS-RhoGEF was not directly measureable, selective knockdown of endogenous *D.m.* Rac1/2 in S2 cells impaired the cell spreading triggered by coexpression of EhRGS-RhoGEF, EhGα1(Q/L), and EhRacC(Q/L), suggesting that *Drosophila* Rac may serve as a substrate for EhRGS-RhoGEF in a cellular context. However, the cell spreading experiments provide limited insight into the precise signaling mechanics. For instance, additional cellular factors may contribute to EhRGS-RhoGEF activation, and we cannot rule out the possibility that overexpressed *E. histolytica* signaling components promote cell spreading through other endogenous signaling pathways.

In isolation, EhRGS-RhoGEF appears to adopt an autoinhibited conformation, with direct obstruction of the presumptive Rho substrate-binding surface by a putative inhibitory helix and its DH and PH domain interactions. We hypothesize that binding of EhGα1·GTP and EhRacC·GTP to EhRGS-RhoGEF, possibly together with other cellular context factors, such as membrane localization or posttranslational modifications, may lead to a structural rearrangement of the putative inhibitory helix and the PH domain, allowing for substrate Rho GTPase binding and nucleotide exchange. The predicted mode of EhRGS-RhoGEF autoinhibition, as derived from the crystal structure, is comparable to that of mammalian PDZ-RhoGEF, seen in solution

 ©2013 Elsevier Ltd All rights reserved

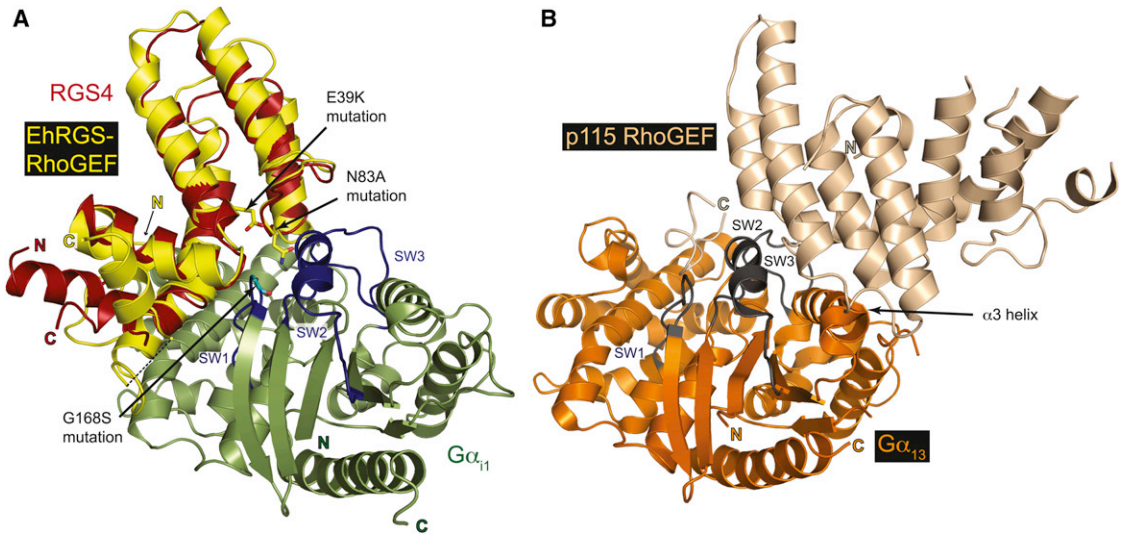

Figure 7. Evolutionary Analysis of the EhGα1/EhRGS-RhoGEF Signaling Pathway

Canonical RGS domains, illustrated by RGS4 (PDB 1AGR), and rgRGS domains of mammalian RGS-RhoGEFs, represented by that of p115 (PDB 3AB3), exhibit distinct folds.

(A) The EhRGS-RhoGEF RGS domain structure (yellow) closely resembles RGS4 (red), suggesting a canonical Gα/RGS domain interaction as exhibited by the RGS4/$G\alpha_{i1}$ complex. Canonical RGS domains engage primarily switches 1 and 2, while rgRGS domains interact with the effector interface of $G\alpha_{12/13}$ (orange) family members, primarily through switch 2 and the α3 helix, although the N-terminal extension required for GAP activity also contacts the three switch regions and the all-helical domain (B). The EhGα1(G168S), EhRGS-RhoGEF(E39K), and EhRGS-RhoGEF(N83A) mutations can distinguish between the two modes of binding by selectively disrupting the canonical RGS domain binding site. Divergence of EhGα1 sequence from known mammalian subfamilies, together with the canonical nine-helix RGS domain of EhRGS-RhoGEF and its mode of EhGα1 interaction, suggest that the EhGα1/RGS-RhoGEF signaling axis arose by an evolutionary mechanism distinct from and functionally convergent with that of the mammalian $G\alpha_{12/13}$/RGS-RhoGEF axis.

Figure S6 contains a comparison of EhGα1 to mammalian Gα subfamily members.

studies (Zheng et al., 2009). However, in the case of PDZ-RhoGEF, an acidic stretch of its rgRGS-DH domain linker interacts with a DH domain surface basic cluster, distinct from the inhibitory helix interface seen here in the crystal structure of EhRGS-RhoGEF. The rgRGS-DH linker of p115 RhoGEF also apparently inhibits the GEF activity of its DH-PH domain tandem, although both SAXS analyses and crystallographic studies of the DH-PH domains with short segments of the linker intact suggest a different linker disposition than that seen in EhRGS-RhoGEF (Chen et al., 2011). The RGS-DH linker in EhRGS-RhoGEF is >100 residues shorter than those of mammalian homologs (Figure S1C), further suggesting that this region does not have a conserved structure across species.

Endogenous EhRGS-RhoGEF likely represents a functional signaling link between heterotrimeric G-proteins and Rho family GTPases in *E. histolytica*. Indeed, Rho GTPases and other Dbl family RhoGEFs in *E. histolytica* are also known to regulate multiple processes important for pathogenesis, such as actin reorganization during chemotaxis, surface receptor capping, cell killing, phagocytosis, and tissue destruction (Guillén, 1996). A surprisingly large family of Rho GTPases (>20 members) is apparently simultaneously expressed in the single-celled parasite (Bosch et al., 2011a). Further studies are needed to determine which Rho family members are activated by EhRGS-RhoGEF and what downstream signaling pathways are utilized.

Overexpression of EhRGS-RhoGEF resulted in reduced *E. histolytica* trophozoite chemotactic migration, attachment to and killing of host cells, and secretion of cysteine proteases. By each of these measures, the EhRGS-RhoGEF trophozoite strain phenocopies a strain overexpressing a dominant negative EhGα1 point mutant and exhibits an opposing trend to trophozoites overexpressing wild-type EhGα1 (Bosch et al., 2012), consistent with ectopically overexpressed EhRGS-RhoGEF serving to accelerate GTP hydrolysis on EhGα1 and thus inhibit its signaling. Given the amenability of heterotrimeric G protein signaling to pharmacological manipulation (Gilchrist, 2007), this pathway provides a promising drug target for the treatment of amoebic colitis.

EXPERIMENTAL PROCEDURES

Cloning and Protein Purification

See Supplemental Experimental Procedures.

Crystallization and Structure Determination

Crystals of the full-length EhRGS-RhoGEF (aa 1–519) yielded diffraction data not suitable for either molecular replacement or anomalous dispersion. However, by removing two residues on both the N- and C-termini of EhRGS-RhoGEF, we obtained another crystal form with improved diffraction quality, ultimately allowing structure determination by SAD. Crystallization was achieved by hanging drop vapor diffusion at 18°C. EhRGS-RhoGEF at 15 mg/ml in crystallization buffer (50 mM 4-(2-hydroxyethyl)-1-piperazineethanesulfonic acid [HEPES] pH 7.5, 100 mM NaCl, and 1 mM dithiothreitol) was mixed 1:1 and equilibrated against crystallization solution containing 16% (w/v) polyethylene glycol 3350 and 100 mM sodium malonate pH 5.0. Hexagonal plate crystals grew to 400 × 150 × 20 μm over 5 days. EhRGS-RhoGEF crystals displayed the symmetry of space group C2 (a = 86.1 Å, b = 46.3 Å, c = 142.6 Å, $\alpha = \gamma = 90°$, $\beta = 104.2°$), with one monomer in the asymmetric unit. Prior to data collection, crystals were cryoprotected in crystallization solution supplemented with 25% (v/v) glycerol.

Anomalous diffraction data were obtained at 0.97954 Å wavelength (selenium absorption peak) and 100 K temperature at the GM/CA-CAT ID-D beamline (APS, Argonne National Labs) and processed using HKL2000 (Otwinowski and Minor, 1997). A highly redundant data set was obtained combining partial data sets from five points along the EhRGS-RhoGEF plate crystal. Heavy atom searching identified eight of eight possible sites, and refinement yielded an estimated Bayes correlation coefficient of 48.2 to 2.5 Å resolution. After density modification, the estimated Bayes correlation coefficient increased to 66.0. Approximately 75% of the model was constructed automatically, and the remaining portion was built manually. The current model (Table 1) contains one EhRGS-RhoGEF monomer.

Refinement was carried out against peak anomalous data with Bijvoet pairs kept separate using phenix.refine (Adams et al., 2010) interspersed with manual model revisions using the program Coot (Emsley and Cowtan, 2004) and consisted of conjugate-gradient minimization and calculation of individual atomic displacement and translation/libration/screw parameters (Painter and Merritt, 2006). Residues that could not be identified in the electron density were: 1, 139, 140, 153–156, and 452–454. The model exhibits excellent geometry, as determined by MolProbity (Chen et al., 2010a). A Ramachandran analysis identified 97.6% favored, 2.4% allowed, and 0% disallowed residues. Coordinates and structure factors are deposited in the RCSB Protein Data Bank (4GOU).

Single Turnover Nucleotide Hydrolysis

GTP hydrolysis by single turnover assays was quantified as previously described (Bosch et al., 2011b). For GTPase acceleration assays, increasing concentrations of purified EhRGS-RhoGEF were added along with the hydrolysis-initiating magnesium.

Surface Plasmon Resonance

Optical detection of protein binding was conducted as described previously (Kimple et al., 2010). Briefly, His_6-tagged wild-type or mutant EhRGS-RhoGEF was immobilized on an nitrilotriacetic acid (NTA) chip surface by capture coupling and increasing concentrations of wild-type EhGα1, and mutants were flowed over at 10 μl/s in various nucleotide states. In complementary experiments, glutathione S-transferase (GST)-EhGα1 was immobilized on an anti-GST chip surface, as described (Hutsell et al., 2010), and increasing concentrations of EhRGS-RhoGEF and mutants flowed over.

NTA Affinity Coprecipitation

See Supplemental Experimental Procedures.

Trophozoite Stable Transfection

See Supplemental Experimental Procedures.

Chemotactic Migration

Trophozoite migration assays were performed essentially as described previously (Gilchrist et al., 2008). Briefly, amoebae harvested in log growth phase were suspended in serum-free trypticase yeast extract iron growth medium and 50,000 cells loaded in the upper chamber of a Transwell migration chamber (Costar, 8 μm pore size). The lower chamber contained growth medium with or without 15% adult bovine serum. Transwell plates were incubated at 37°C for 2 hr under anaerobic conditions (GasPak EZ, BD Biosciences).

Host Cell Attachment

Attachment of *E. histolytica* trophozoites to epithelial monolayers was assessed as previously described (Shrimal et al., 2010). CHO cells were grown to confluency in 24 well plates, washed, and fixed in 4% paraformaldehyde for 30 min. Trophozoites (3×10^5) were added to the fixed monolayers in medium 199 supplemented with 5.7 mM cysteine, 1 mM ascorbic acid, and 25 mM HEPES (pH 6.9). After incubation at 37°C for 30 min, each well was washed gently two times with warm PBS to remove unattached trophozoites. Monolayer-attached trophozoites were quantified by counting with an inverted microscope. Each experiment was performed in quadruplicate and statistical significance determined by Student's t test.

Cell Killing

Killing of mammalian cells (Jurkat) was assessed using the CytoTox-ONE membrane integrity assay (Promega). In 96-well plates, 5×10^5 Jurkat cells and/or 2.5×10^5 trophozoites were incubated at 37°C in 200 μl of medium 199 (Sigma) supplemented with 5.7 mM cysteine, 0.5% BSA, and 25 mM HEPES pH 6.8. After 2 hr, 50 μl of medium from each well was incubated with Cytotox reagent, and a colorimetric measure of extracellular lactate dehydrogenase activity was obtained after 10 min. Each experiment was performed in quadruplicate and statistical significance determined by Student's t test.

Cysteine Protease Activity

See Supplemental Experimental Procedures.

S2 Cell Culture and Spreading Assay

S2 cells were obtained from the *Drosophila* Genome Resource Center (Bloomington, IL), and cultivated as described previously (Rogers and Rogers, 2008). S2 cells were maintained in SF900 SFM (Invitrogen, Carlsbad, CA) and transfected with 2 μg total DNA using the Amaxa nucleofector system (Lonza, Basel, Switzerland). Expression of transfected constructs was induced with 35 μM $CuSO_4$. Double-stranded RNAs (see Supplemental Experiment Procedures for primers) were produced using a Promega (Madison, WI) Ribomax T7 kit according to manufacturer instructions. S2 cells at 50%–90% confluency in six-well plates were treated every other day for 7 days with 7.5 μg/ml of double-stranded RNA. On day 5 of RNA interference (RNAi) treatment, cells were transfected as above and then induced on day 6. Cells were resuspended and plated on poly-L-lysine (Sigma-Aldrich, St. Louis, MO)-coated coverslips and allowed to spread for 1 hr. For quantifying numbers of cells with spreading, each condition was repeated at least three times and $\geq$100 cells were counted per experiment.

Immunofluorescence Microscopy

See Supplemental Experimental Procedures.

SUPPLEMENTAL INFORMATION

Supplemental Information includes one table, six figures, and Supplemental Experimental Procedures and can be found with this article online at http://dx.doi.org/10.1016/j.str.2012.11.012.

ACKNOWLEDGMENTS

We thank Dr. William Petri (UVa) for provision of *E. histolytica* genomic DNA and RNA and Dr. Michael Miley (UNC) for crystallographic assistance. Crystallographic data were collected at the Advanced Photon Source (Argonne National Labs) 23-IDD beamline. This work was supported by NIH grant GM082892 (to D.P.S.); an NIGMS MSTP award (T32 GM008719) and individual F30 NRSA fellowships MH074266 (to A.J.K.); and DK091978 (to D.E.B.).

Received: June 24, 2012
Revised: November 20, 2012
Accepted: November 20, 2012
Published: December 20, 2012

REFERENCES

Adams, P.D., Afonine, P.V., Bunkóczi, G., Chen, V.B., Davis, I.W., Echols, N., Headd, J.J., Hung, L.W., Kapral, G.J., Grosse-Kunstleve, R.W., et al. (2010). PHENIX: a comprehensive Python-based system for macromolecular structure solution. Acta Crystallogr. D Biol. Crystallogr. *66*, 213–221.

Aittaleb, M., Boguth, C.A., and Tesmer, J.J. (2010). Structure and function of heterotrimeric G protein-regulated Rho guanine nucleotide exchange factors. Mol. Pharmacol. *77*, 111–125.

Bielnicki, J.A., Shkumatov, A.V., Derewenda, U., Somlyo, A.V., Svergun, D.I., and Derewenda, Z.S. (2011). Insights into the molecular activation mechanism of the RhoA-specific guanine nucleotide exchange factor, PDZRhoGEF. J. Biol. Chem. *286*, 35163–35175.

Bosch, D.E., Wittchen, E.S., Qiu, C., Burridge, K., and Siderovski, D.P. (2011a). Unique structural and nucleotide exchange features of the Rho1 GTPase of Entamoeba histolytica. J. Biol. Chem. *286*, 39236–39246.

Bosch, D.E., Kimple, A.J., Sammond, D.W., Muller, R.E., Miley, M.J., Machius, M., Kuhlman, B., Willard, F.S., and Siderovski, D.P. (2011b). Structural determinants of affinity enhancement between GoLoco motifs and G-protein alpha subunit mutants. J. Biol. Chem. *286*, 3351–3358.

Bosch, D.E., Kimple, A.J., Muller, R.E., Giguère, P.M., Machius, M., Willard, F.S., Temple, B.R., and Siderovski, D.P. (2012). Heterotrimeric G-protein signaling is critical to pathogenic processes in Entamoeba histolytica. PLoS Pathog. *8*, e1003040.

Chen, V.B., Arendall, W.B., 3rd, Headd, J.J., Keedy, D.A., Immormino, R.M., Kapral, G.J., Murray, L.W., Richardson, J.S., and Richardson, D.C. (2010a). MolProbity: all-atom structure validation for macromolecular crystallography. Acta Crystallogr. D Biol. Crystallogr. *66*, 12–21.

Chen, Z., Singer, W.D., Sternweis, P.C., and Sprang, S.R. (2005). Structure of the p115RhoGEF rgRGS domain-Galpha13/i1 chimera complex suggests convergent evolution of a GTPase activator. Nat. Struct. Mol. Biol. *12*, 191–197.

Chen, Z., Medina, F., Liu, M.Y., Thomas, C., Sprang, S.R., and Sternweis, P.C. (2010b). Activated RhoA binds to the pleckstrin homology (PH) domain of PDZ-RhoGEF, a potential site for autoregulation. J. Biol. Chem. *285*, 21070–21081.

Chen, Z., Guo, L., Sprang, S.R., and Sternweis, P.C. (2011). Modulation of a GEF switch: autoinhibition of the intrinsic guanine nucleotide exchange activity of p115-RhoGEF. Protein Sci. *20*, 107–117.

Chen, Z., Guo, L., Hadas, J., Gutowski, S., Sprang, S.R., and Sternweis, P.C. (2012). Activation of p115-RhoGEF requires direct association of Gα13 and the Dbl homology domain. J. Biol. Chem. *287*, 25490–25500.

Das, B., Shu, X., Day, G.J., Han, J., Krishna, U.M., Falck, J.R., and Broek, D. (2000). Control of intramolecular interactions between the pleckstrin homology and Dbl homology domains of Vav and Sos1 regulates Rac binding. J. Biol. Chem. *275*, 15074–15081.

Emsley, P., and Cowtan, K. (2004). Coot: model-building tools for molecular graphics. Acta Crystallogr. D Biol. Crystallogr. *60*, 2126–2132.

Ferguson, K.M., Kavran, J.M., Sankaran, V.G., Fournier, E., Isakoff, S.J., Skolnik, E.Y., and Lemmon, M.A. (2000). Structural basis for discrimination of 3-phosphoinositides by pleckstrin homology domains. Mol. Cell *6*, 373–384.

Gilchrist, A. (2007). Modulating G-protein-coupled receptors: from traditional pharmacology to allosterics. Trends Pharmacol. Sci. *28*, 431–437.

Gilchrist, C.A., Baba, D.J., Zhang, Y., Crasta, O., Evans, C., Caler, E., Sobral, B.W., Bousquet, C.B., Leo, M., Hochreiter, A., et al. (2008). Targets of the Entamoeba histolytica transcription factor URE3-BP. PLoS Negl. Trop. Dis. *2*, e282.

González De la Rosa, C.H., Arias-Romero, L.E., de Jesús Almaraz-Barrera, M., Hernandez-Rivas, R., Sosa-Peinado, A., Rojo-Domínguez, A., Robles-Flores, M., and Vargas, M. (2007). EhGEF2, a Dbl-RhoGEF from Entamoeba histolytica has atypical biochemical properties and participates in essential cellular processes. Mol. Biochem. Parasitol. *151*, 70–80.

Guillén, N. (1996). Role of signalling and cytoskeletal rearrangements in the pathogenesis of Entamoeba histolytica. Trends Microbiol. *4*, 191–197.

Hutsell, S.Q., Kimple, R.J., Siderovski, D.P., Willard, F.S., and Kimple, A.J. (2010). High-affinity immobilization of proteins using biotin- and GST-based coupling strategies. Methods Mol. Biol. *627*, 75–90.

Kimple, A.J., Muller, R.E., Siderovski, D.P., and Willard, F.S. (2010). A capture coupling method for the covalent immobilization of hexahistidine tagged proteins for surface plasmon resonance. Methods Mol. Biol. *627*, 91–100.

Kimple, A.J., Bosch, D.E., Giguère, P.M., and Siderovski, D.P. (2011). Regulators of G-protein signaling and their Gα substrates: promises and challenges in their use as drug discovery targets. Pharmacol. Rev. *63*, 728–749.

Lan, K.L., Sarvazyan, N.A., Taussig, R., Mackenzie, R.G., DiBello, P.R., Dohlman, H.G., and Neubig, R.R. (1998). A point mutation in Galphao and Galphai1 blocks interaction with regulator of G protein signaling proteins. J. Biol. Chem. *273*, 12794–12797.

Meigs, T.E., Juneja, J., DeMarco, C.T., Stemmle, L.N., Kaplan, D.D., and Casey, P.J. (2005). Selective uncoupling of G alpha 12 from Rho-mediated signaling. J. Biol. Chem. *280*, 18049–18055.

Meza, I., Talamás-Rohana, P., and Vargas, M.A. (2006). The cytoskeleton of Entamoeba histolytica: structure, function, and regulation by signaling pathways. Arch. Med. Res. *37*, 234–243.

Oldham, W.M., and Hamm, H.E. (2008). Heterotrimeric G protein activation by G-protein-coupled receptors. Nat. Rev. Mol. Cell Biol. *9*, 60–71.

Otwinowski, Z., and Minor, W. (1997). Processing of X-ray Diffraction Data Collected in Oscillation Mode. In Methods in Enzymology, C.W. Carter, Jr., ed. (New York: Academic Press), pp. 307–326.

Painter, J., and Merritt, E.A. (2006). Optimal description of a protein structure in terms of multiple groups undergoing TLS motion. Acta Crystallogr. D Biol. Crystallogr. *62*, 439–450.

Petri, W.A., Jr., Haque, R., and Mann, B.J. (2002). The bittersweet interface of parasite and host: lectin-carbohydrate interactions during human invasion by the parasite Entamoeba histolytica. Annu. Rev. Microbiol. *56*, 39–64.

Ralston, K.S., and Petri, W.A., Jr. (2011). Tissue destruction and invasion by Entamoeba histolytica. Trends Parasitol. *27*, 254–263.

Rogers, S.L., and Rogers, G.C. (2008). Culture of Drosophila S2 cells and their use for RNAi-mediated loss-of-function studies and immunofluorescence microscopy. Nat. Protoc. *3*, 606–611.

Rogers, S.L., Wiedemann, U., Stuurman, N., and Vale, R.D. (2003). Molecular requirements for actin-based lamella formation in Drosophila S2 cells. J. Cell Biol. *162*, 1079–1088.

Rossman, K.L., and Sondek, J. (2005). Larger than Dbl: new structural insights into RhoA activation. Trends Biochem. Sci. *30*, 163–165.

Shrimal, S., Bhattacharya, S., and Bhattacharya, A. (2010). Serum-dependent selective expression of EhTMKB1-9, a member of Entamoeba histolytica B1 family of transmembrane kinases. PLoS Pathog. *6*, e1000929.

Snyder, J.T., Worthylake, D.K., Rossman, K.L., Betts, L., Pruitt, W.M., Siderovski, D.P., Der, C.J., and Sondek, J. (2002). Structural basis for the selective activation of Rho GTPases by Dbl exchange factors. Nat. Struct. Biol. *9*, 468–475.

Soundararajan, M., Willard, F.S., Kimple, A.J., Turnbull, A.P., Ball, L.J., Schoch, G.A., Gileadi, C., Fedorov, O.Y., Dowler, E.F., Higman, V.A., et al. (2008). Structural diversity in the RGS domain and its interaction with heterotrimeric G protein alpha-subunits. Proc. Natl. Acad. Sci. USA *105*, 6457–6462.

Suzuki, N., Nakamura, S., Mano, H., and Kozasa, T. (2003). Galpha 12 activates Rho GTPase through tyrosine-phosphorylated leukemia-associated RhoGEF. Proc. Natl. Acad. Sci. USA *100*, 733–738.

Tesmer, J.J., Berman, D.M., Gilman, A.G., and Sprang, S.R. (1997). Structure of RGS4 bound to AlF4—activated G(i alpha1): stabilization of the transition state for GTP hydrolysis. Cell *89*, 251–261.

WHO (1997). WHO/PAHO/UNESCO report. A consultation with experts on amoebiasis. Mexico City, Mexico 28-29 January, 1997. Epidemiol. Bull. *18*, 13–14.

Zheng, M., Cierpicki, T., Momotani, K., Artamonov, M.V., Derewenda, U., Bushweller, J.H., Somlyo, A.V., and Derewenda, Z.S. (2009). On the mechanism of autoinhibition of the RhoA-specific nucleotide exchange factor PDZRhoGEF. BMC Struct. Biol. *9*, 36.